Colloid & Polymer Science Colloid & Polymer Sci. **261**, 1022–1030 (1983)

COLLOID SCIENCE

Determination of micelle structure and charge by neutron small-angle scattering

J. B. Hayter and J. Penfold

Institut Laue-Langevin, Grenoble, France and
Neutron Division, Rutherford and Appleton Laboratory, Chilton, Didcot, Oxon. U. K.

Abstract: We present a general method of determining the structure and charge of globular ionic micelles, using neutron small-angle scattering. The micellar solutions may have any concentration within the micellar phase. The method is based in part on an analytic calculation of the interparticle correlations between monodisperse spherical micelles, and we discuss the theory in some detail to justify its application to polydisperse globular particles. Experimental results are presented for several cationic and anionic micellar systems.

Key words: micelle structure, micelle charge, neutron scattering

1. Introduction

In a earlier study of sodium dodecyl sulphate (SDS) micelles [1], we showed that it was possible to analyse neutron small-angle scattering data from concentrated micellar solutions, using the methods of liquid theory to handle the intermicellar correlations [2]. Two features emerged from that study. First, although a general three-shell micelle geometry was used, the experimental results showed that a two-shell model was in fact sufficient; for SDS, we found that the outer (polar) shell thickness corresponded to about 1.5 headgroup diameters, indicating a surface roughness on the scale of a few tenths of a nm. Secondly, the data was extremely well fitted by a model with only two parameters (aggregation number and net charge), despite a theoretical description which assumed the micelles were monodisperse spheres. The same analytical method has since been applied to a number of other concentrated micellar systems [3–6] and found to work very well in all cases.

In the present paper, we first address the question of why a theory based on monodisperse spheres works so well for systems which are unlikely in detail to be either monodisperse or perfectly spherical. To this end, we shall outline the derivation of the fundamental scattering relation in a way designed to emphasize the inherent assumptions; we shall show that the latter are not in fact restrictive for charged micelles. In particular, the main effect of not too large deviations from sphericity or monodispersity will be shown to be the addition of a diffuse background to the scattered intensity, which may be modelled and subtracted from the data. We shall then discuss the use of a general two-shell model for (nearly) spherical micelles. Finally we give some experimental details, in particular the use of absolute scaling, and present as examples of the application of the method results on sodium dodecyl sulphate (SDS), dodecyltrimethylammonium chloride (C_{12}TACl) and bromide (C_{12}TABr) and hexadecyltrimethylammonium chloride (C_{16}TACl). The earlier SDS results have been re-analysed in terms of the present two-shell model and new measurements at lower concentrations have been analysed, using a recent rescaling extension of the liquid theory on which the analysis is based [7].

The results on SDS confirm our earlier conclusions. In contrast, we find a much lower degree of surface roughness for the alkyl-trimethylammonium micelles.

2. Theory

The scattering of a slow neutron by a nucleus is characterized by a single parameter, b, the nuclear scattering length. The neutron-nuclear interaction occurs over a distance very much smaller than the neutron wavelength λ, so the scattered wave is spherical. If the momenta of incident and scattered waves are

k_i and k_f, respectively, a wave scattered by a nucleus at a point r in the sample will thus be phase-shifted with respect to scattering at the origin by a phase-factor exp $(i\ Q.r)$, where $Q = k_i - k_f$ is the momentum transferred in the scattering process. ($Q = (4\pi/\lambda) \sin\theta$ for elastic scattering through angle 2θ).

Numerous texts are available on the general theory of neutron scattering [see, e.g. 8–11] and we shall restrict the present discussion to a clarification of those features strictly relevant to the problem of small-angle scattering from charged micelles. In particular, this means that we shall be concerned with calculating the *coherent* super-position of scattered waves, and we shall assume the data has been corrected for incoherent scattering due to isotopic and nuclear spin effects, as well as for multiple scattering and absorption (see section 3). The relevant differential scattering cross-section, σ, per unit solid angle, Ω, is thus calculated from a straightforward summation of amplitude-weighted phase-shifts

$$\left(\frac{d\sigma}{d\Omega}\right)_{\mathrm{COH}} = < | \sum_j \bar{b}_j \exp(iQ \cdot R_j) |^2 > \qquad (1)$$

where the bar on the scattering length indicates that the value has been averaged over the isotopic and nuclear spin distribution of each atomic species, and R_j is the position of the atom relative to an arbitrary origin in the sample. (The *bound* scattering length should be used, since the momentum transfer is small in forward scattering; the present calculation would of course apply equally well to X-ray or light scattering provided the nuclear scattering lengths $\bar{b}$ were replaced by the appropriate electronic form-factors.) The sum is over all atoms in the sample, and $<>$ represents an average over all possible configurations of atoms, which for the systems under consideration may be taken as a classical ensemble average; we shall also use $<>_Q$ to denote averaging over particle orientations with respect to the direction of Q.

2.1 Separation of intermicellar from intramicellar scattering

We now take advantage of the fact that the relative positions of certain sets of atoms in the sample are constrained by the requirement that they form a micelle. It is then convenient to include this specifically by writing all atomic positions in a given micelle relative to its geometric centre, so that (1) becomes

$$\left(\frac{d\sigma}{d\Omega}\right)_{\mathrm{COH}} = < \sum_{n,m} \sum_{j(n)} \sum_{k(m)} \bar{b}_j \bar{b}_k \exp(iQ \cdot r_{j,k}) > \qquad (2)$$

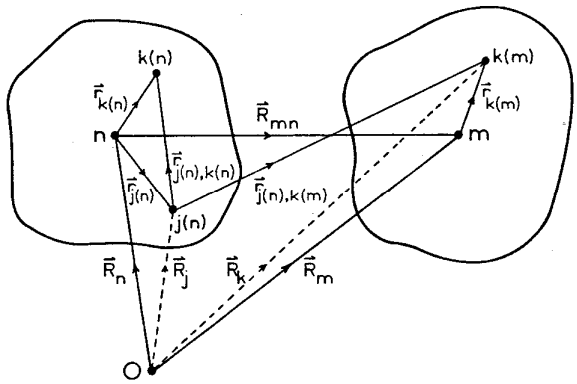

Fig. 1. Geometrical notation used to specify inter- and intramicellar relationships (see text)

where $j \equiv j(n)$ refers to the j'th atom in the n'th micelle and $r_{j,k}$ is the relative separation of two atoms. Then (see fig. 1)

$$r_{j(n),k(m)} = R_{mn} + r_{k(m)} - r_{j(n)}$$

where m,n refer in general to different micelles separated by a centre-to-centre distance R_{mn}. Equation (2) thus separates naturally into intermicellar ($m \neq n$) and intramicellar ($m = n$) terms:

$$\left(\frac{d\sigma}{d\Omega}\right)_{\mathrm{COH}} = < \sum_{j(n)} \sum_{k(n)} \bar{b}_j \bar{b}_k \exp[iQ \cdot (r_j - r_k)] >$$

$$+ < \sum_{n \neq m} \exp(iQ \cdot R_{mn}) \sum_{j(n)} \sum_{k(m)} \bar{b}_j \bar{b}_k \exp[iQ \cdot (r_k - r_j)] > \qquad (3)$$

We first assume for the sake of clarity that all micelles have the same shape and size; the effect of polydispersity will be discussed later. The first term to be averaged in (3) is than just N times the square of the single-micelle form-factor, defined as

$$F(Q) = \sum_{j(n)} \bar{b}_j \exp(iQ \cdot r_j) \qquad (4)$$

where N is the number of micelles, the sum is over all atoms in the micelle and the distances are relative to the micelle centre.

The first term in (3) is calculable for any specified micelle geometry. The second term, however, cannot be evaluated without further specifying the probabilities (a) that the micelles are separated by a given distance R_{mn}, and (b) that at that distance they have the particular relative orientation specified by $r_{k(m)} -$

$r_{j(n)}$. Here the strong electrostatic repulsion between charged micelles comes to our aid, since it makes close contact unlikely between neighbouring micelles. Provided the micelles are relatively globular, strong correlation of orientation due to steric effects will thus occur only rarely, and over the centre-to-centre distances usually encountered there will be little correlation between orientation and intermicellar distance. (Since a sphere has no orientation, such correlations are of course rigorously absent in the case of spherical micelles). The sum over orientations in the second term of (3) (indices j and k) then no longer depends on the intermicellar distance, $\boldsymbol{R}_{mn}$, and the sums may be averaged separately:

$$\left(\frac{d\sigma}{d\Omega}\right)_{\mathrm{COH}} = N < |F(Q)|^2 >_Q + < \sum_{n \neq m} \exp\,(i\boldsymbol{Q}\cdot\boldsymbol{R}_{mn}) > < \sum_{j(n)} \sum_{k(m)} \bar{b}_j\, \bar{b}_k \exp\,[i\boldsymbol{Q}\cdot(\boldsymbol{r}_k - \boldsymbol{r}_j)] >$$

Further, under the above assumption, multipolar terms in the interaction potential will be dominated by the Coulombic (zero-order) term, so that any angular dependence will be relatively weak. The intermicellar potential will thus be an effectively central potential over the distances of interest, and hence the orientations $\boldsymbol{r}_{k(m)}$ and $\boldsymbol{r}_{j(n)}$ will be statistically independent, so that finally we may write

$$\left(\frac{d\sigma}{d\Omega}\right)_{\mathrm{COH}} = N < |F(Q)|^2 >_Q + < \sum_{n \neq m} \exp\,(i\boldsymbol{Q}\cdot\boldsymbol{R}_{mn}) > < \sum_{j(n)} \bar{b}_j \exp\,(i\boldsymbol{Q}\cdot\boldsymbol{r}_j) >_Q^2$$

where we have used the fact that the sign of Q is irrelevant when averaging over all orientations. The term involving different micelles ($n \neq m$) is just $N[S(Q)-1]$, where the intermicellar structure factor $S(Q)$ is defined as

$$S(Q) = N^{-1} < \sum_{nm} \exp\,(i\boldsymbol{Q}\cdot\boldsymbol{R}_{mn}) > = 1 + N^{-1} < \sum_{n \neq m} \exp\,(i\boldsymbol{Q}\cdot\boldsymbol{R}_{mn}) >$$

The coherent differential scattering cross-section for monodisperse globular charged micelles is thus to a good approximation

$$\left(\frac{d\sigma}{d\Omega}\right)_{\mathrm{COH}} = N[S(Q) \cdot < F(Q) >_Q^2 + \Delta(Q)] \quad (5)$$

where

$$\Delta(Q) = < |F(Q)|^2 >_Q - < F(Q) >_Q^2 \quad (6)$$

has the familar form of a mean square deviation. In a monodisperse system, $\Delta(Q)$ is identically zero for spheres, and will be small for nearly spherical globular micelles. However, we shall see below that such a term will be non-zero, even for spherical micelles, if the size distribution is polydisperse. Note that this *coherent* disorder term is "switched on" by the correlations, and its effect disappears when the system is sufficiently dilute ($S(Q) = 1$).

In principle, the introduction of polydispersity into the above analysis requires us to return to (3) and to take specific account of an added complication, namely correlations between micelle size and position. In the case of uncharged hard spheres, for example, the calculations of van Beurten and Vrij [12] show that this can be a particularly important effect. In a very real sense, however, hard spheres represent a pathological case when discussing particle suspensions, since their packing is determined *only* by geometrical considerations. That is, the only potential in the system (the hard-sphere potential) is infinite and hence independent of temperature. Contact between hard spheres is highly probable in a dense system, so that in a polydisperse mixture a small sphere is likely to be found, for example, in the "cage" formed by a cluster of larger spheres. This is very different from the pair distribution found for charged spheres, when close contact is a most unlikely configuration because of the strong electrostatic repulsion. (If this were not the case, the suspension would no longer be stable). Thus, not only are clusters energetically unfavorable when the particles are charged, but a smaller sphere whose charge had the same sign would be unlikely to enter any "cage" so formed, and indeed similarly charged spheres of any size would be repelled.

In an electrostatically stabilized real colloidal suspension, therefore, it is reasonable to assume that correlations between particle size and position are very much weaker than would be the case in a sterically stabilized suspension of equivalent polydispersity. Equation (5) should thus remain a good approximation for polydisperse charged globular mi-

celles, provided neither the polydispersity nor the asphericity is too large, with the disorder term $\Delta(Q)$ effectively accounting for the deviations from monodisperse spherical particles. Returning to (6), the disorder due to polydispersity among spherical particles becomes

$$\Delta(Q) = \sum_m p_m | < F_m(Q) >_Q - \bar{F}(Q) |^2 \qquad (7)$$

where p_m is the (normalised) probability of finding a micelle with form-factor $F_m(Q)$, and the mean (size-averaged) form factor is

$$\bar{F}(Q) = \sum_n p_n < F_n(Q) >_Q$$

$$= \sum_n p_n \sum_{j(n)} \bar{b}_j \sin(Qr_j)/(Qr_j) \qquad (8)$$

Here we have used the fact that $<F_m(Q)>_Q^2 = <F_m^2(Q)>_Q$ for any given sphere, and we have written the angular average of (4) explicitly. The disorder term (7) is thus a sum of non-negative Fourier components with similar amplitudes but a wide distribution of phases, and we expect it to exhibit no sharp Q-dependent structure. (This is analogous to the well-known coherent diffuse scattering due to defects in solid materials [13]. It is also similar in nature to the term which gives rise to the diffuse background now considered important in light scattering [14]). In the systems we shall consider, $\Delta(Q)$ is numerically very small, but if necessary it may be calculated using a model distribution function. The intensity function of interest, $I(Q)$, may thus be derived from the measured cross-section (per micelle) as

$$I(Q) \equiv P(Q)\, S(Q)$$

$$= N^{-1}(d\sigma/d\Omega)_{\mathrm{COH}} - \Delta(Q) \qquad (9)$$

where the size-averaged scattering function $P(Q) = |\bar{F}(Q)|^2$. Note the difference between the approximation we propose and the form used for hard-spheres by van Beurten and Vrij [12], who defined an *effective* $\bar{S}(Q)$ multiplying a mean scattering factor $\sum p_n <F_n^2(Q)>_Q$. Our result corresponds to writing down the coherent part of their equation (1) with the assumption that their interference function H_{ik} is independent of i and k for not too polydisperse (paucidisperse) charged systems.

Equation (9) is the central result which allows $P(Q)$ to be obtained from the measured scattering cross-section $(d\sigma/d\Omega)_{\mathrm{COH}}$. The data is first placed on an absolute scale (see section 3). $P(Q)$ is modelled by taking a suitable geometry for the micelle; we discuss a typical spherical geometry in the next section. $S(Q)$ may then be calculated for a given micellar charge, following Hayter and Penfold [2] and Hansen and Hayter [7]. The structural parameters and charge are then refined by fitting the product $P(Q)S(Q)$ to the derived intensity $I(Q)$, using a standard least-squares procedure; in a polydisperse system, the standard deviation of particle sizes may also be a fitting parameter, with $\Delta(Q)$ re-evaluated at each cycle of the fit.

2.2 Model calculation of $P(Q)$

In the case of single-chain surfactants comprising a paraffin chain $CH_3(CH_2)_n$, a headgroup ($HG^{\pm}$) and a counterion ($CI^{\mp}_{+}$), we have found that the two-shell model of figure 2 works generally very well over the globular micelle range. In its simplest form, the model replaces individual monomer configurations by a conceptual "average monomer". The latter is characterised by having its methyl group and a fraction α of its methylenes inside a dry core of radius R_1. The remaining methylenes, the ***hydrated*** headgroups and any non-ionized ***hydrated*** counterions are distributed uniformly in the outer layer, while the methyl distribution in the inner core is taken as random. Refinements such as Dill-Flory [15] or Gruen [16] distributions of methyls are easily incorporated, as are ellipsoidal deformations and polydisperse size averaging [see, e.g. 5]. We have found in practice, however, that the present experiments (which do not use specific isotopic substitution to mark sites) are described

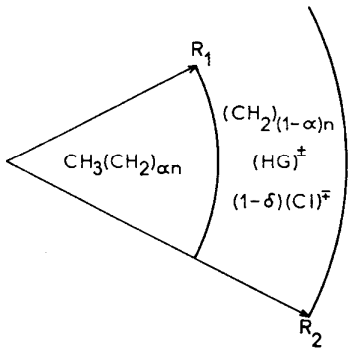

Fig. 2. Mean disposition of a surfactant molecule $CH_3(CH_2)_n(HG)^{\pm}(CI^{\mp})$ in a two-shell micelle of mean radii R_1 and R_2. HG = headgroup; CI = counterion, δ = degree of ionisation. Both HG and CI are assumed to carry hydration shells. Note that even when the micelle is *physically* smooth, it may be *chemically* rough; that is, the outer shell is filled but headgroups may be found at varying distances from the centre.

within error by the simple liquid-like centre. This point is discussed by Hayter and Zemb [3], and we only remark here that the use of nearly random core packing to calculate the scattering does not necessarily imply a liquid core. The indistinguishability of carbons from different chains means that a mixture, for example, having mostly radial order for some chains and substantial tangential order for others will not be distinguished from a different arrangement of *bonds* which leads to about the same arrangement of *nuclei*.

Two important features of the model are worth discussing. The first is that when $R_1 = l_c$, the length of the hydrocarbon chain, α may still be less than unity. Tanford [17] has argued that the micelle must then be ellipsoidal. Provided the major-to-minor axial ratio is within the range of order 0.8–1.2, numerical calculations show that it is experimentally very difficult to distinguish such a shape from an equivalent sphere after isotropic averaging. A good fit to the model thus indicates globularity within, say, 20% of spherical, rather than true sphericity. We note, however, that micelles may contain more monomers than would correspond to $R_1 = l_c$ with $\alpha = 1$ (see below) without becoming highly elliptical; approximate sphericity may be maintained by absorbing new monomers onto a small micelle with some degree of tangential order in the chains [3]; that is, by a "wrapping" process.

The second feature is that the micelle described by the average sphere may be rough, in the sense described in [1]. The parameter which indicates a rough micelle is the distance $r = R_2 - R_1$. If r is equal to the diameter of a headgroup, the micelle is smooth; if it is larger, we interpret that to mean a rough disposition of headgroups within the shell of thickness r. In all cases, the inner sphere of radius R_1 is considered smooth.

As an example of the calculation of the micelle geometry for a given aggregation number ν and a given degree of ionisation δ, we consider the simplest case of the average spherical micelle. The parameters required are the volume V_{HG} and hydration number w_{HG} of the headgroup, together with the corresponding values V_{CI} and w_{CI} for the counterion. We first calculate the radius of the sphere which would contain *all* of the hydrocarbon:

$$R_h = [3\nu(V_{CH_3} + n\,V_{CH_2})/4\pi]^{1/3} \tag{10}$$

where V_{CH_3} and V_{CH_2} are the volume of the methyl and methylene groups, respectively. If $R_h \leqslant l_c$ we set $\alpha = 1$ and take $R_1 = R_h$. Otherwise, we set $R_1 = l_c$ and calculate

$$\alpha = (V_1 - \nu V_{CH_3})/n\nu V_{CH_2} \tag{11}$$

where $V_1 = 4\pi R_1^3/3$. From the total volume

$$V_2 = \nu[V_{CH_3} + nV_{CH_2} + V_{HG} + w_{HG}\,V_S + (1-\delta)(V_{CI} + w_{CI}\,V_S)] \tag{12}$$

we obtain $R_2 = (3V_2/4\pi)^{1/3}$, where V_S is the volume of a solvent molecule in the headgroup or counterion hydration shell.

Once the geometry and contents of each shell is thus specified, the calculation of $P(Q)$ proceeds as described in [1]. For more complicated models leading to elliptical geometry, appropriate formulae are given in [18]. If desired, $P(Q)$ may also be averaged over a distribution of sizes. We have taken [17]

$$l_c = 0.2765 + 0.1265n\ \text{nm} \tag{13}$$

and have used for the other parameters the values given in table 1.

2.3 A note on the use of Guinier plots

In the absence of interactions ($S(Q) = 1$) the scattering function at very small Q may be written in the well-known Guinier form

$$(d\sigma/d\Omega) \propto \exp(-Q^2R_g^2/3) \tag{14}$$

where R_g is the radius of gyration of the particle [19]. In micellar solutions near the cmc, the Guinier plot ($\log(d\sigma/d\Omega)$ vs Q^2) is often found to be linear, and it is tempting to draw the conclusion that interactions are therefore absent. For the case of μ-emulsions, Cebula et al. [20] have noted that this need not be correct. We wish to emphasize here that the problem is general. As a straightforward example we consider the case of low-Q scattering from monodisperse spherical micelles interacting through a screened Coulomb potential. Such a potential is *tempered*; that is, it

Table 1. Volumes (V) and hydration numbers (w, where applicable) used in the data analysis

i	V_i/nm^3	w_i
CH_3	0.0543	
CH_2	0.0248	
SO_4^-	0.0606	5
$N^+(CH_3)_3$	0.1023	1
Na^+	0.0136	6
Cl^-	0.0289	4
Br^-	0.0393	4
D_2O	0.0302	
H_2O	0.0299	

decays faster than any power of the distance. It can be shown quite generally [21] that for *any* tempered potential, $S(Q)$ has no linear term, so that at small Q

$$S(Q) = S_1 + S_2 Q^2 + \ldots \quad (15)$$

Expanding (14) and using (5) and (15) then yields

$$(d\sigma/d\Omega) \propto \exp\{[(S_2/S_1) - R_g^2/3]Q^2\} \quad (16)$$

to second order in Q, so that the Guinier plot remains linear, but the slope is no longer a direct measure of the radius of gyration. Since $S_2/S_1 > 0$ for a tempered repulsive potential, the radius of gyration will be underestimated by a Guinier analysis if interactions are present.

The effect can be dramatic, even for small interactions, and it is worth following Cebula et al. [20] and evaluating a numerical example. Consider the limit of weak interaction, namely uncharged micelles, so that only excluded volume effects are present. For a volume fraction of 1%, expanding $S(Q)$ [2] at small Q yields $S_1 = 0.92$ and $S_2 = 0.008\ \sigma^2$, where σ is the (spherical) micelle diameter. The corresponding radius of gyration is 0.387σ, and the Guinier slope predicted by (16) is $-0.041\ \sigma^2$. The use of (14) to interpret this slope would yield an apparent radius of gyration of 0.352σ; that is, excluded volume effects alone would cause the radius to be underestimated by nearly 10% at a volume fraction of only 0.01. For charged micelles similar effects would be noted at even lower volume fractions.

3. Experimental

Solutions were prepared in D_2O (98.7%, I.L.L. Grenoble) using Eastman analytic grade SDS, C_{12}TACl, C_{12}TABr and C_{16}TACl as starting materials. Merck analytic grade NaCl or NaBr was used as appropriate to make solutions of variable ionic strength. All measurements in the present series were taken at 313 ± 2K using standard quartz cells of 1mm or 2mm optical path. Measurements were performed on the neutron camera D17 at the I.L.L., using incident wavelengths λ of 1.0 or 1.2 nm ($\Delta\lambda/\lambda = 0.1$) with a sample-to-detector distance of 1.4m. Other conditions were as described in [1]. Measurements were made in the range $Q < 0.25\ \text{nm}^{-1}$.

Data were corrected for absorption, background, solvent scattering, detector efficiency and incoherent scattering from the sample, using standard techniques [22]. After all corrections, the intensity was found to decay to a small, flat level at the higher momentum transfers. This level, which was generally less than 1% of the peak intensity, was taken as a measure of $\Delta(Q)$. Although the latter will exhibit some Q-dependence in our experimental range, we considered that the small absolute value observed justified the approximation of taking $\Delta(Q)$ as flat in these experiments, and this level was merely subtracted from the data. The excellent results obtained (see section 4) provide *a posteriori* justification of this procedure.

All measurements were converted to absolutely scaled cross-sections ($d\sigma/d\Omega$) using light water as a standard [23]. Although the statistical precision of the raw data is better than 1%, this scaling procedure involves a number of quantities whose precision is of a similar order, and the final *absolute* scale is estimated to be not better than 10%.

4. Results and discussion

Typical fully corrected scattered intensity data is plotted in figure 3. We have chosen to show a low surfactant concentration to emphasize that there is still considerable interaction present even in this relatively dilute system, due to the long range of the Coulombic effects. The data was fitted using the model discussed in section 2. In calculating $P(Q)$ a number of systematic errors enter the final absolute scale, mainly due to lack of precision in the scattering length densities. Although the molar volume of, say, the hydrocarbon chain is well-known, the separate contributions of the methyl and methylene groups to the local scattering length density can be less well estimated. For a given model, these systematic errors result in uncertainties in the predicted absolute theoretical intensity of the same order as those in the measured absolute intensity. The fitting procedure takes these errors into account by first performing a least-squares refinement on an *arbitrary* scale. The factor by which the absolute theory must be multiplied to match the absolutely scaled data is then calculated. Ideally, this factor should be unity. In view of the various systematic errors discussed above and in section 3, we accept the fit to a given model if (a) the fit converges within statistical error, and (b) the ratio of absolute scales beween theory and experiment is within 30% of unity.

The result of this procedure is plotted in figure 3, with the separate contributions from $P(Q)$ and $S(Q)$ shown as dashed lines. We emphasize the utility of absolute scaling, even at the level of precision quoted.

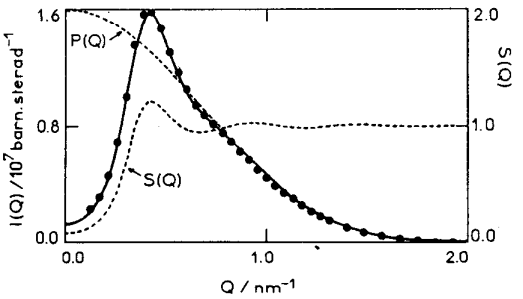

Fig. 3. Measured (•) and fitted (−) values of $I(Q) = P(Q)S(Q)$ as a function of momentum transfer Q for 0.03 M C_{16}TACl in D_2O. Note the structure in $S(Q)$ due to charge interactions even at this relatively low surfactant concentration.

Table 2. Fitted aggregation number (ν) and degree of ionisation (δ) for SDS solutions at the surfactant and salt concentration shown. The derived inner (R_1) and outer (R_2) radii and average number of waters of hydration per monomer (w_{av}) are also tabulated

[SDS] mol.dm^{-3}	[NaCl] mol.dm^{-3}	ν	δ	R_1 nm	R_2 nm	w_{av}
0.016	0.0	77	0.30	1.67	2.32	9.2
0.04	0.0	88	0.30	1.67	2.42	9.2
	0.05	107	0.28	1.67	2.59	9.3
	0.2	120	0.20	1.67	2.71	9.8
0.07	0.0	88	0.34	1.67	2.32	9.0
0.10	0.0	98	0.24	1.67	2.53	9.6
	0.05	109	0.25	1.67	2.61	9.5
	0.1	117	0.24	1.67	2.68	9.6
	0.2	126	0.21	1.67	2.75	9.7
0.40	0.0	120	0.22	1.67	2.70	9.7
	0.05	130	0.20	1.67	2.77	9.8
	0.1	138	0.19	1.67	2.85	9.8
	0.2	146	0.19	1.67	2.90	9.9
0.50	0.0	122	0.19	1.67	2.71	9.9
0.60	0.05	128	0.20	1.67	2.77	9.8
	0.1	135	0.18	1.67	2.82	9.9

On an arbitrary scale a number of models may fit the data with, say, different degrees of headgroup hydration. Absolute scaling usually allows one restricted set of parameters to be chosen. As further confirmation, we have also calculated the scattering from the model particle under different contrast conditions (e.g. H_2O/D_2O mixture as solvent) and compared these predictions with experiment at several contrasts for each of several of the concentrations studied. Good agreement was obtained on an absolute scale without any adjustment of the model parameters. This, in particular, tends to confirm that the level of hydration chosen is correct, since altering the solvent scattering length density concomitantly alters the scattering power of the hydrated parts of the micelle. Tables 2, 3, 4 and 5 summarise the results on the four surfactants. The average hydration number per monomer is calculated from

$$w_{av} = w_{HG} + (1-\delta)\, w_{Cl} \qquad (17)$$

Table 3. Parameters for $C_{12}TACl$; notation as for table 2

[C_{12}TACl] mol.dm^{-3}	[NaCl] mol.dm^{-3}	ν	δ	R_1 nm	R_2 nm	w_{av}
0.2	0.0	60	0.31	1.67	2.01	3.8
	0.1	60	0.33	1.67	2.00	3.7
0.4	0.0	59	0.36	1.67	1.99	3.6
	0.1	61	0.36	1.67	2.00	3.6
0.6	0.0	67	0.30	1.67	2.08	3.8
	0.1	67	0.28	1.67	2.07	3.9

Table 4. Parameters for $C_{12}TABr$; notation as for table 2

[C_{12}TABr] mol. dm^{-3}	[NaBr] mol. dm^{-3}	ν	δ	R_1 nm	R_2 nm	w_{av}
0.05	0.0	57	0.33	1.64	1.97	3.7
0.10	0.0	68	0.24	1.67	2.12	4.0
0.20	0.0	69	0.29	1.67	2.12	3.9
	0.1	76	0.17	1.67	2.21	4.0
0.40	0.0	75	0.24	1.67	2.19	4.0
	0.1	78	0.16	1.67	2.23	4.1
0.60	0.0	75	0.24	1.67	2.19	4.1
	0.1	82	0.15	1.67	2.27	4.1

It will be noted that the aggregation numbers for 0.04 and 0.1 M SDS are somewhat smaller than previously quoted [1]. In the original analysis, the approximation used to calculate $S(Q)$ was no longer strictly valid at the lowest volume fractions involved. This theoretical restriction has now been removed [7] and $S(Q)$ may be calculated reliably at any volume fraction.

Near the CMC, the SDS micelles are small and smooth, as indicated by the thickness ($R_2 - R_1$) of the polar layer. At higher concentrations this layer becomes thicker, indicating the development of a rough surface in the sense discussed in section 2.2. We interpret the growth as being due to absorption of monomers onto existing micelles as the concentration increases; these new monomers probably "wrap" onto the existing structure rather than penetrating radially.

The situation is quite different for the dodecyltrimethylammonium surfactants, which form almost smooth micelles. For these compounds the size is much less dependent on either surfactant or salt concentration than is the case for SDS. This may indicate an optimal packing geometry for this combination of chain length and headgroup, since the hexadecyltrimethylammonium monomer again shows

Table 5. Parameters for $C_{16}TACl$; notation as for table 2

[C_{16}TACl] mol. dm^{-3}	[NaCl] mol. dm^{-3}	ν	δ	R_1 nm	R_2 nm	w_{av}
0.03	0.0	90	0.28	2.10	2.43	3.9
0.05	0.0	92	0.28	2.11	2.45	3.9
	0.1	119	0.34	2.17	2.65	3.6
0.10	0.0	91	0.33	2.10	2.43	3.7
	0.1	116	0.27	2.17	2.65	3.9
0.20	0.0	109	0.24	2.17	2.60	4.0
	0.1	119	0.20	2.17	2.68	4.2
0.40	0.0	116	0.20	2.17	2.68	4.2
	0.1	121	0.21	2.17	2.69	4.1
0.60	0.0	120	0.23	2.17	2.68	4.1
	0.1	125	0.19	2.17	2.73	4.0

a tendency to grow with increased concentration. The latter micelles are also slightly rough at higher concentrations; as noted earlier, the present experiments do not attempt to distinguish this geometry from a smoother but slightly elliptical shape.

The qualitative difference between the SDS and TMA micelles is also apparent in the parameter α, the average fraction of methylenes which are in a totally dry environment. Near the cmc, α is effectively unity for all of the cationic compounds, and at the highest concentrations studied about 80% of the methylenes are still in a dry environment. For SDS, however, α is of order 0.7 even near the cmc, and it drops to 0.4 at high concentration, suggesting a much less well-defined core/polar interface in the anionic micelles compared with the alkyltrimethylammonium compounds.

The diffuse term $\Delta(Q)$ was small but non-zero for all the systems studied, increasing with concentration. We have not made a detailed analysis of the values, but numerical calculations suggest it corresponds to size polydispersity typically of order 15%. (Discussions of the effects of polydispersity on scattering from *dilute* systems may be found in [28, 29]. In cases where the polydispersity is thought to be large (> 20%), we would recommend using a full model calculation of $\Delta(Q)$ but in our relatively paucidisperse system the subtraction of the residual flat level (discussed in section 3) seems a satisfactory procedure.

5. Conclusion

We have presented arguments justifying the use of a theory of correlations between charged spheres in a screening medium to interpret scattering data from solutions of charged globular micelles. Application of the method to small-angle neutron scattering data yields aggregation numbers and degrees of ionisation. Analysis of experimental data shows that a two-shell model is generally applicable to data on nearly spherical micelles, the thickness of the outer shell relative to the headgroup size characterising the micelle roughness. We find that SDS micelles are rough (on the scale of several tenths of a nm) in concentrated solution. In contrast, dodecyltrimethylammonium halide micelles are smaller and smoother, indicating that this monomer may represent optimal packing. Hexadecyltrimethylammonium chloride micelles are intermediate between the previous cases.

The values of aggregation number, charge and size derived from the present scattering experiments are generally consistent with those reported in the extensive literature [see e.g. 24–27]. The results indicate that the micellar systems studied are relatively paucidisperse (polydispersity $\lesssim 20\%$). They also confirm that our assumption of weak correlation between size and position is reasonable for the present systems. It is hard to place limits on this assumption *a priori*; we recommend using it where it appears justified by the results. The fact that it works very well for charged micelles, but rather less well for charged polystyrene spheres [31] may indicate that some charge compensation mechanism is operational in the micellar systems, so that particles of slightly different sizes may have similar interaction potentials at short range.

We believe the present technique has a number of advantages over those previously used, especially now that access to neutron small-angle scattering spectrometers is becoming relatively widespread. The method is experimentally straightforward, data collection is rapid and interpretation of the data is now well understood. The analytical method is applicable to X-ray, light or neutron scattering data measured on systems at any concentration, and a number of applications has recently been reported [3–6, 30].

Acknowledgement

We are indebted to Drs. S. W. Lovesey and P. N. Pusey for critical comments on Section 2 of the manuscript.

References

1. Hayter, J. B., J. Penfold, J. Chem. Soc. Faraday Trans. I, **77**, 1851 (1981).
2. Hayter, J. B., J. Penfold, Molec. Phys. **42**, 109 (1981).
3. Hayter, J. B., T. Zemb, Chem. Phys. Lett. **93**, 91 (1982).
4. Johnson, J. S., L. J. Magid, R. Triolo, G. D. Wignall, W. C. Koehler, NCSASR Report of Activities (Oak Ridge National Laboratory, 1982).
5. Bendedouch, D., S. H. Chen, W. C. Koehler, J. S. Lin, J. Chem. Phys. **76**, 5022 (1982).
6. Hayter, J. B., M. Zulauf, Colloid and Polymer Sci. **260**, 1023 (1982).
7. Hansen, J. P., J. B. Hayter, Molec. Phys. **46**, 651 (1982).
8. Marshall, W., S. W. Lovesey, "Theory of Thermal Neutron Scattering" (Clarendon Press, Oxford, 1971).
9. Bacon, G. E., "Neutron Scattering in Chemistry" (Butterworths, London, 1977).
10. Lovesey, S. W., T. Springer, eds., "Dynamics of Solids and Liquids by Neutron Scattering" (Springer, Berlin, 1977).
11. Dachs, H., ed., "Neutron Diffraction" (Springer Berlin, 1978).
12. van Beurten, P., A. Vrij, J. Chem. Phys. **74**, 2744 (1981).
13. Lovesey, S. W., in ref. [10], pp. 17–22.
14. Pusey, P. N., H. M. Fijnaut, A. Vrij, J. Chem. Phys. **77**, 4270 (1982).
15. Dill, K. A., P. J. Flory, Proc. Natl. Acad. Sci. U. S. **78**, 676 (1981).
16. Gruen, D. W. R., J. Colloid Interface Sci. **84**, 281 (1981).
17. Tanford, C., J. Phys. Chem. **76**, 3020 (1972).
18. Kostorz, G., ed., "Neutron Scattering in Materials Science" (Academic, New York, 1979).